

Purification and characterization of a stimulator of plasmin generation from the antiangiogenic agent Neovastat: identification as immunoglobulin kappa light chain

Dominique Boivin, Mathieu Provençal, Sébastien Gendron, David Ratel, Michel Demeule, Denis Gingras, Richard Béliveau*

Laboratoire de médecine moléculaire, Hôpital Sainte-Justine-UQAM, Centre de cancérologie, Charles-Bruneau, Centre de Recherche de l'Hôpital Sainte-Justine, 3175, Chemin Côte-Sainte-Catherine, Montreal, Que., Canada H3T 1C5

Received 14 June 2004, and in revised form 23 August 2004

Available online 25 September 2004

Abstract

We have recently shown that Neovastat, an antiangiogenic extract from shark cartilage, stimulates the *in vitro* activation of plasminogen by facilitating the tissue-type plasminogen activator (tPA)-dependent conversion of plasminogen to plasmin. In this report, we describe the purification and characterization of the stimulatory molecules. Neovastat was subjected to a three-step purification procedure including gel filtration, preparative isoelectric focusing, and preparative SDS-PAGE. Two 28-kDa proteins with *pI*s of approximately 4.5 and 6.5 were purified to apparent homogeneity and identified as immunoglobulin (Ig) kappa light chains by N-terminal microsequencing. Ig light chains do not directly stimulate the activity of tPA or plasmin, suggesting a mechanism of action involving an interaction with plasminogen. Kinetic analysis showed that both Ig light chains accelerate the *in vitro* tPA-dependent conversion of plasminogen in plasmin by increasing the affinity of tPA for plasminogen by 32- and 38-fold (K_m decrease from 456 nM to 12–14 nM). Shark Ig light chains also stimulated the degradation of fibrin by the tPA/plasminogen system in an *in vitro* assay. A direct interaction between Ig light chains and plasminogen ($K_A = 4.0\text{--}5.5 \times 10^7 \text{ M}^{-1}$; $K_D = 18\text{--}25 \text{ nM}$) and with tPA ($K_A = 2.8 \times 10^7 \text{ M}^{-1}$; $K_D = 36 \text{ nM}$) was demonstrated using real time binding measured by surface plasmon resonance. Ig light chain is the first molecule associated with the antiangiogenic activity of Neovastat to be purified and identified.

© 2004 Elsevier Inc. All rights reserved.

Keywords: Neovastat; AE-941; Angiogenesis; Endothelial cells; Immunoglobulin; Shark cartilage; Plasminogen activator

Tumor-induced angiogenesis play an important role in the growth, progression, and metastasis of tumors [1]. In the process of angiogenesis, endothelial cells are stimulated by tumor-derived angiogenic factors, such as basic fibroblast growth factor (bFGF)¹ and vascular endothelial growth factor (VEGF), leading to increased

proliferation, extracellular matrix degradation and formation of new blood vessels in the vicinity of the tumor cells [2]. Several studies support that proteolytic degradation of the extracellular matrix (ECM) by both matrix metalloproteinases (MMPs) and plasminogen activators/plasminogen systems play an important role in angiogenesis [3].

The plasminogen activator (PA)/plasmin system comprises two major types of PA, tissue-type PA (tPA) and urokinase PA (uPA) that both specifically convert circulating plasminogen to the active proteinase plasmin by cleavage of the Arg⁵⁶¹–Val⁵⁶² peptide bond [4]. Plasmin is a trypsin-like protease with broad

* Corresponding author. Fax: +1 514 345 2359.

E-mail address: molmed@justine.umontreal.ca (R. Béliveau).

URL: <http://www.unites.uqam.ca/oncomol/>.

¹ Abbreviations used: tPA, tissue-type plasminogen activator; uPA, urokinase plasminogen activator; Ig, immunoglobulin; Plg, plasminogen.

specificity that is capable of degrading most components of the ECM either directly or through activation of MMPs or elastases [5]. While uPA and tPA share a common substrate, there is evidence that the physiological roles of the two proteins are distinct. The binding of uPA to its cell-surface receptor (uPAR) is involved in pericellular proteolysis and is associated with cell locomotion [4,6]. Interference with the binding of uPA to its receptor results in an inhibition of tumor angiogenesis [7] thus suggesting that uPA/uPAR interaction plays an important role in neovascularization. In contrast, the role of tPA in angiogenesis remains unclear. tPA is mainly synthesized in endothelial cells where it is stored in Weibel–Palade bodies and released following stimulation of the cells by several stimuli [8]. The released tPA is a key enzyme in fibrinolysis due to its ability to significantly increase the cleavage of fibrin-bound plasminogen into plasmin, leading to fibrin degradation [4]. How this fibrinolytic activity contributes to angiogenesis remains unknown.

We have recently reported that Neovastat, a shark cartilage extract with antiangiogenic properties, activate enzymes of the fibrinolytic system, i.e., the tPA-dependent activation of plasminogen to plasmin [9]. We proposed that Neovastat, through stimulation of plasminogen activation, might induce a localized degradation of the fibrin matrix, which is often found surrounding “leaky” tumor-associated blood vessels [10], thereby blocking or reducing tumor angiogenesis. Although fibrinolysis is generally associated with the promotion of angiogenesis, there is considerable evidence that some components of the PA/plasminogen system may inhibit angiogenesis. Recently, plasmin has been suggested to be involved in the generation of anti-angiogenic proteins, such as angiostatin [11], and therefore to play an additional role in the angiogenesis cascade. Moreover, high tPA levels correlate with good prognosis in various tumors [12,13] whereas lower tPA levels have been associated with malignant tumors [14]. While such a positive role of tPA in tumor progression remains unexplained, it has been proposed that the overstimulation of plasmin generation by tPA may induce the degradation of the pro-angiogenic fibrin matrix, resulting in the inhibition of angiogenesis [15].

Neovastat is a naturally occurring inhibitor of angiogenesis derived from shark cartilage (dogfish) [16]. Based on results from Phase II clinical trials [17,18], this compound is currently undergoing Phase III clinical trials for the treatment of non-resectable non-small cell lung cancer [18]. There is now considerable evidence that the pharmacological properties of Neovastat are associated with the presence of multiple angiogenesis inhibitors, including inhibitors of MMP activities [19] and of VEGF-mediated signaling events [20], as well as to the presence of an endothelial-specific pro-apoptotic activity [21]. These antiangiogenic activities are likely to be

responsible for the antitumor and antimetastatic properties of Neovastat observed in in vivo models [22].

In this work, we have purified and identified from Neovastat the molecules that stimulate plasminogen activator activity. We found that in vitro, purified shark immunoglobulin kappa light chain markedly stimulates tPA activity and that this stimulation is due to a direct interaction with plasminogen and tPA, resulting in an increased catalytic efficiency of tPA-mediated plasmin generation.

Experimental procedures

Materials

Neovastat (AE-941) was obtained from Æterna Laboratories (Québec City, Que., Canada) [23]. Human recombinant single-chain tPA was from Calbiochem (San Diego, CA). [Glu]Plasminogen, the plasmin-specific substrate Chromozym PL (tosyl-glycyl-prolyl-lysine-4-nitroanilide acetate) and the tPA substrate Chromozym tPA (*N*-methylsulfonyl-*D*-phenylalanyl-glycyl-arginine-4-nitroanilide acetate) were from Roche Biochemicals (Laval, Que., Canada). Plasminogen-free human fibrinogen was from Calbiochem (La Jolla, CA) and ¹²⁵I-labeled human fibrinogen was from Amersham Biosciences (Baie d’Urfée, Que., Canada). Plasmin, and other biochemical reagents were from Sigma (St. Louis, MO). Sensor chips (CM5) were from BIAcore (Piscataway, NJ).

Gel filtration chromatography

Desalted and lyophilized shark cartilage extract (4.8 g) (Neovastat) was resuspended in 40 ml buffer S (20 mM Tris–HCl, pH 8.0, 100 mM NaCl, and 0.1 mM EDTA) and centrifuged at 40,000g, 30 min. Two milliliters of the resulting Neovastat solution (about 30 mg protein/ml) was applied to a semi-preparative Superdex 75 gel filtration column (Pharmacia) pre-equilibrated with buffer S, and was eluted at a flow rate of 1.2 ml/min. Four-milliliter fractions were collected, dialyzed overnight against 20 mM Tris–HCl, pH 8.0, and 20- μ l aliquots were assayed for plasminogen activation activity. A total of 19 distinct separations were performed on the Superdex 75 column. The most active fractions were pooled and concentrated using an Ultra-free-15 (5000 Da cut-off) centrifugal filter device (Millipore).

Preparative isoelectric focusing

The Rotofor unit was operated according to the manufacturer instructions (Bio-Rad). Briefly, samples were mixed with ampholytes (Bio-Rad, 2% final concentra-

tion) in 2% CHAPS, 4 M urea, and 10 mM DTT and immediately injected in the Mini Rotofor sample chamber. The anode buffer was 0.1 M H₃PO₄ and the cathode buffer was 0.1 M NaOH. The power supply was set at 12 W constant power and the run was stopped when the voltage reached a constant value (2000–2400 V). Twenty fractions were collected and NaCl was added to a final concentration of 1 M in order to strip ampholytes from proteins. Fractions were extensively dialyzed (five changes over 2 days) against 20 mM Tris–HCl, pH 8.0, using 6000–8000 MWCO dialysis tubing.

Preparative gel electrophoresis

The concentrated active pool fraction from preparative isoelectric focusing was further purified by preparative gel electrophoresis. A Bio-Rad Prep Cell apparatus model 491 was used following manufacturer's instructions, and using the discontinuous Laemmli SDS–PAGE buffer system. Approximately 2–5 mg of protein in 2.5 ml was applied to a 12.5% polyacrylamide separating gel (3.7 cm diameter × 10 cm long) with a 1.5 cm 4% polyacrylamide stacking gel. The lower chamber tank buffer was recirculated through the cooling core of the apparatus at about 100 ml/min and electrophoresis was performed at 60 mA constant current. After about 6–8 h, when the bromophenol blue dye begins to elute, 190 fractions of 2 ml were collected at an elution rate of 0.5 ml/min. Every fifth fraction collected was dialyzed extensively (six changes over 2 days) against 20 mM Tris–HCl, pH 8.0, and 20- μ l aliquots were assayed for plasminogen activation activity. 20- μ l aliquots were also analyzed on 15% mini-gels.

Plasminogen activation assay

The kinetics of tPA- and uPA-mediated plasminogen activation was determined by measuring amidolytic activity of the plasmin generated by activation of plasminogen. The reaction was performed at 25 °C in a final volume of 200 μ l with 158 μ M Chromozym PL, 138 nM [Glu]Plasminogen, and 5.13 nM tPA or uPA, in a buffer consisting of 50 mM Tris–HCl (pH 7.4), 100 mM NaCl, and 5 mM CaCl₂. Plasmin generation was monitored at 405 nm for 1 h using a thermostatically controlled Molecular Devices microplate reader (SpectraMax Plus) connected to a Macintosh computer. Under these conditions, if a constant rate of plasminogen activation is assumed, the concentration of plasmin increases linearly with time and that of *p*-nitroaniline follows a parabolic curve [24]. Initial rates of plasmin generation were calculated using linear regression analysis of plots of $A_{405 \text{ nm}}$ versus time², as described [24].

For the measurement of plasmin activity, similar conditions were used except that tPA and plasminogen were omitted from the buffer and the reaction was started by

the addition of plasmin. tPA amidolytic activity was measured under these conditions using Chromozym tPA as the tPA substrate.

Kinetic analysis

The steady-state rate of plasminogen activation, i.e., the tPA turnover number (k) was calculated at different plasminogen concentrations using values of initial rates of plasmin generation ($A_{405 \text{ nm}}/\text{min}^2$) and the equation:

$$k = A_{405 \text{ nm}}/0.5\Delta\epsilon_{405}k_1[\text{tPA}]t^2, \quad (1)$$

where $\Delta\epsilon_{405} = 10,500$, $[\text{tPA}] = 1 \text{ nM}$ and k_1 , the plasmin turnover number = 8.5 s^{-1} [25]. Nonlinear regression analysis of the data was performed using the GraphPad Prism 4.0a software (GraphPad Software, San Diego, CA, USA).

In vitro fibrinolysis assay

In a 96-wells plate, fibrin gel (3 mg/ml final concentration) was prepared by mixing 5 μ l of plasminogen-free human fibrinogen (6 mg/ml) containing 0.05 μ Ci [¹²⁵I]fibrinogen (178 μ Ci/mg fibrinogen) with 5 μ l of human thrombin solution (2 U/ml final concentration). The gels were incubated at 37 °C for 30 min to allow complete gelling. After washing, 100 μ l of EBM-2 media (Clontec) containing various tested proteins [tPA (5 nM), plasminogen (325 nM), Ig 4.5 or Ig 6.5 (2.5 μ g/ml), aprotinin (0.4 mg/ml)] was added on top of the fibrin gel. After a 10 min incubation at 37 °C, solubilized iodinated fibrin degradation products released in the media were quantified by γ -scintillation counting.

BIAcore analysis

Real time protein–protein interactions were examined on a BIAcore instrument (BIAcore X). tPA or plasminogen was immobilized on different flow cells of a CM5 sensor chip using an amine-coupling kit (Amersham Biosciences). Briefly, the chip surface was first activated by injection of 35 μ l of 1:1 mixture of 0.4 M *N*-ethyl-*N'*-(dimethylaminopropyl) carbodiimide hydrochloride and 0.1 M *N*-hydroxysuccinimide. tPA and plasminogen (50 μ g/ml) in 20 mM acetate buffer pH 4.0 and 5.5, respectively, were immobilized on one flow cell. An additional flow cell was prepared as a blank background by activating it under the same buffer conditions. Remaining activated groups on each flow cell were blocked by injection of 35 μ l of 1 M ethanolamine–HCl, pH 8.5. Using these coupling conditions, about 6000–8000 RU of either tPA or plasminogen were immobilized on the sensor chip surface. Finally, the system was primed with the running buffer (50 mM Tris–HCl, pH 7.5, 150 mM NaCl, and 5 mM CaCl₂).

Purified proteins were diluted in running buffer and were injected at a flow rate of 10 $\mu\text{l}/\text{min}$ and the interaction with the immobilized proteins was monitored over a 10–15 min period. Protein interactions were analyzed using both the Langmuir binding model, which is the simplest model for 1:1 interaction between analyte and immobilized ligand, and a two-state conformational change model that describe a 1:1 binding of analyte to immobilized followed by a conformational change.

Analytical SDS-PAGE and N-terminal sequencing

Protein samples in sample buffer [62.5 mM Tris-HCl (pH 6.8), 100 mM DTT, 10% glycerol, 2% SDS, and 0.1% bromophenol blue] were heated at 100 °C for 3 min and separated on 0.75 mm-thick, SDS-polyacrylamide gels with a MINI-PROTEAN II apparatus (Bio-Rad). The gels were stained with colloidal Coomassie blue or with Silver Stain Plus (Bio-Rad). For N-terminal microsequencing, protein were electroblotted onto sequencing grade PVDF (Bio-Rad, 0.2 μm), briefly stained with 0.1% Coomassie blue R-250 in 50% methanol and then rapidly destained in 50% methanol, 10% acetic acid. Membranes were finally rinsed in deionized H₂O and air dried. N-terminal microsequencing was performed at the Biotechnology Research Institute (Montreal, Que., Canada) sequencing facility.

Protein assay

Protein concentrations were determined using the bicinchoninic protein assay kit (Pierce, Rockford, IL) and BSA as the standard.

Results

Purification and identification of tPA-dependent plasminogen activation stimulatory proteins from Neovastat

We have recently shown that Neovastat, an antiangiogenic agent extracted from shark cartilage, stimulates the *in vitro* activation of plasminogen by facilitating the tPA-dependent conversion of plasminogen to plasmin [9]. In an effort to identify the shark cartilage tPA/plasminogen stimulatory molecules contained in Neovastat we have undertaken their purification. The starting material used for the purification was the macromolecular fraction (1–500 kDa) of Neovastat, obtained by multi-step ultrafiltration. Neovastat was first fractionated by exclusion gel chromatography on a Superdex 75 semi-preparative column, and the activation of plasminogen was determined using an aliquot of each fraction. As shown in Fig. 1, the activity eluted immediately after the column void volume indicating that, under non-denaturing conditions, the activity is

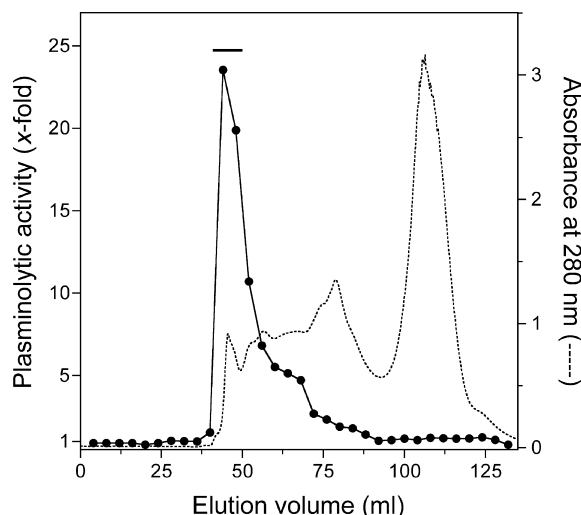


Fig. 1. Fractionation of Neovastat by gel filtration chromatography. Neovastat solution (2 ml) was applied to a semi-preparative Superdex 75 gel filtration column and was eluted at a flow rate of 1.2 ml/min. Four-milliliters of fractions was collected, dialyzed overnight against 20 mM Tris-HCl, pH 8.0, and 20- μl aliquots were assayed for plasminogen activation activity (●). A total of 19 distinct separations were performed on the Superdex 75 column. The most active fractions (bar) were pooled.

associated with a high molecular complex. Using a Superdex 200 analytical FPLC column and appropriate protein standards the native size was estimated to be approx. 340 kDa (data not shown). The most active fractions from the Superdex 75 were pooled and refractionated by isoelectric focusing on a Rotofor apparatus, using a pH 3–10 ampholytes mixture (Fig. 2). Two peaks of activity were obtained (Fig. 2A), the more acidic peak (fractions 2–4) correspond to a *pI* of approx. 4.5, while the other peak (fractions 8–10) migrated with an apparent *pI* of approx. 6.5 (estimated using standard protein with known *pI*s). SDS-PAGE analysis of the fractions (Fig. 2B) shows that cartilage proteins display a wide range of *pI*s and that they could be effectively fractionated by preparative isoelectric focusing using the Rotofor cell. Each peak was individually further purified by preparative SDS-PAGE using the PrepCell apparatus (Fig. 3). The refractionation of both peaks from the Rotofor (Peaks 1 and 2) resulted into two peaks on the PrepCell (Figs. 3A and C). SDS-PAGE analysis of every fifth fraction from the PrepCell showed that peaks 1b and 2b contain a single protein band of about 28 kDa (Figs. 3B and D, fractions 70 and 65, respectively). However, the fractions corresponding to peak 1a and 2a (fractions 10–15 and 5–10, respectively) did not contain any protein stainable by colloidal Coomassie. As these fractions could contain small polypeptides that could not be resolved on a 15% polyacrylamide gel, we re-analyzed these fractions on an 18% polyacrylamide gel, but no peptide was

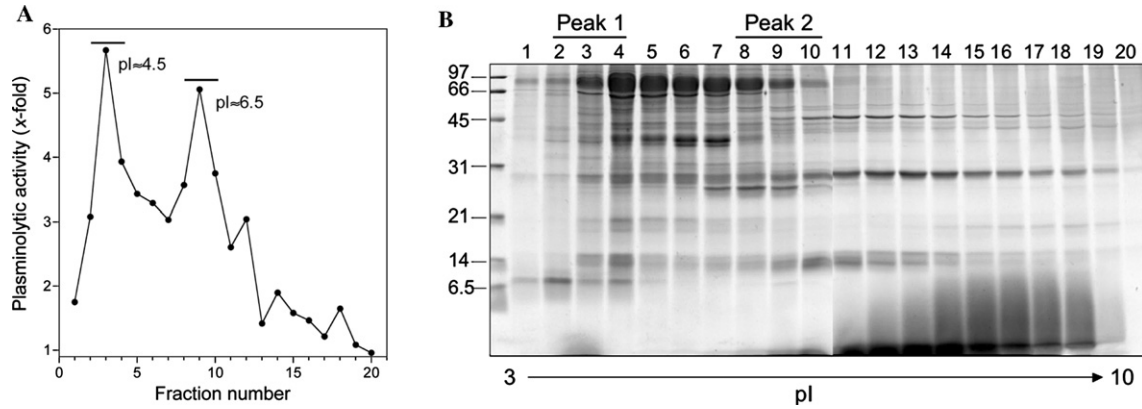


Fig. 2. Preparative isoelectric focusing. Pooled fractions from the Superdex column were dialyzed against 10 mM Tris-HCl, pH 8.0, concentrated, and mixed with 2% ampholytes (pH 3–10), 2% CHAPS, 4 M urea, and 10 mM dithiothreitol. Proteins were focused in the Rotofor mini-chamber at 12 W constant power until the voltage reached a plateau (about 2000–2400 V). Twenty fractions were harvested, adjusted to 1 M NaCl, and dialyzed extensively against 20 mM Tris-HCl, pH 8.0. (A) Aliquots (20 μ l) of the dialyzed fractions were assayed for plasminogen activation activity. (B) Duplicate aliquots were mixed with reducing sample buffer and separated by SDS-PAGE on a 15% polyacrylamide gel. Proteins were stained by colloidal Coomassie. Sizes of molecular weight standard (in kDa) are indicated on the left and the fractions corresponding to peak 1 and 2 are indicated on the top.

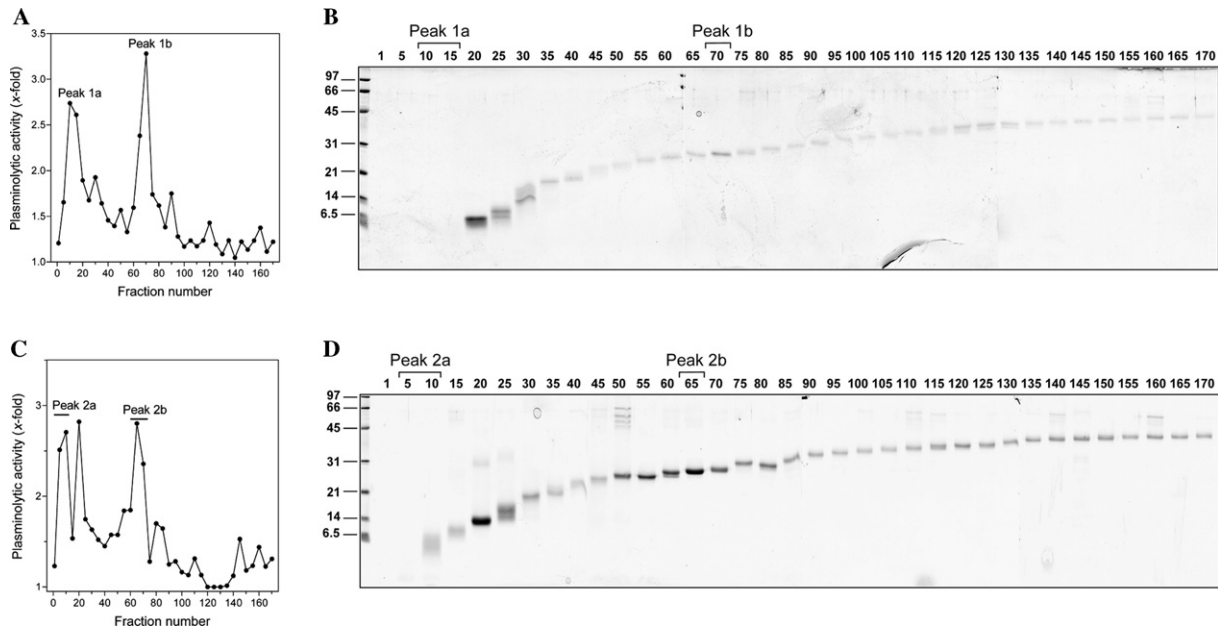


Fig. 3. Preparative SDS-PAGE. Pooled fractions from the Rotofor peak 1 and 2 were individually fractionated on 12.5% polyacrylamide preparative gel. Fractions (2 ml) were collected after the bromophenol blue dye reached the bottom of the gel. One of every fifth fraction was dialyzed extensively to remove excess SDS, dithiothreitol and salts, and then aliquots were used to determine plasminogen activation activity (A and C). Duplicate aliquots were mixed with reducing sample buffer and separated by SDS-PAGE on a 15% polyacrylamide gel. Proteins were stained by colloidal Coomassie (B and D). Sizes of molecular weight standard (in kDa) are indicated on the left and the fractions corresponding to peak 12 are indicated on the top. (A and B) Separation of peak 1 ($pI \approx 4.5$). (C and D) Separation of peak 2 ($pI \approx 6.5$).

detected using a sensitive silver stain reagent (not shown). We thus focused on the identification of the 28-kDa proteins. Fig. 4 shows the polypeptide composition of Neovastat and pooled active fractions after every step of the purification procedure. Purified proteins were electroblotted onto PVDF and sequenced by Edman degradation. N-terminal sequences identified both proteins as immunoglobulin (Ig) kappa light chain

and display a high degree of homology with Ig light chains from various species (Table 1). The 17-amino acid sequence from the p28 with a pI of 6.5 was 100% identical to the N-terminal sequence of nurse shark [26] and the first five amino acids of the other p28 ($pI = 4.5$) were identical, indicating that two Ig light chains were purified and identified. At this point it is not clear what is the molecular basis for the

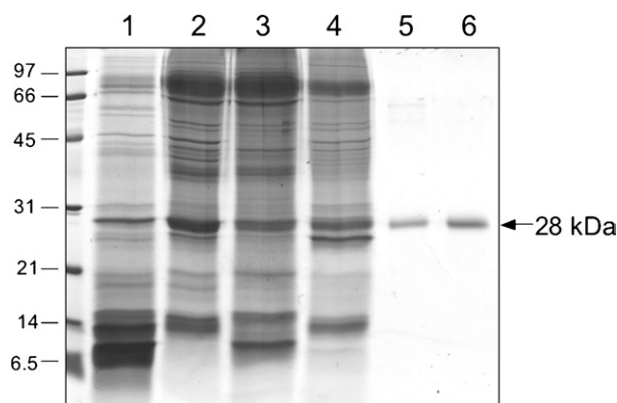


Fig. 4. SDS-PAGE analysis of fractions at different stages of purification. Proteins (20 μ g) from Neovastat (lane 1); Superdex 75 pool (lane 2); Rotofor peak 1b, $pI = 4.5$ (lane; 3); Rotofor peak 2b, $pI = 6.5$ (lane 4), and 0.5 μ g of purified p28 peak 1b (lane 5) or purified p28 peak 2b (lane 6) were analyzed by SDS-PAGE on a 15% polyacrylamide gel. Proteins were stained with colloidal Coomassie. Sizes of molecular weight standard (in kDa) are indicated on the left.

Table 1

Comparison of the N-terminal amino acid sequences of p28 purified proteins with the N-termini of immunoglobulin light chains from various species

DITMT	p28 ($pI = 4.5$)
DITMTQSPFVLSVGLGQ	p28 ($pI = 6.5$)
DITMTQSPFVLSVGLGQ	Nurse shark Ig light chain
TIIMTQSPFALSVTLGQ	Horn shark Ig light chain
DIQMTQSPFSLASLGD	Human Ig light chain
DIVMTQSPFSLAVSLGQ	Mouse Ig light chain

presence of two Ig light chains with different pI s in shark cartilage.

Shark Ig light chains stimulate plasmin generation through an increase in affinity of tPA for plasminogen.

We asked whether or not purified shark Ig light chains directly stimulate either the plasmin or tPA activities by monitoring their effect on the enzyme activities towards synthetic substrates. As shown in Fig. 5, Ig light chains had no effect on both plasmin and tPA activities, whereas they stimulate tPA-dependent plasminogen activation by 7.5-fold. Importantly, Ig light chains had no effect on the uPA-dependent plasmin generation from plasminogen. Mouse Ig light chains from commercial source were also able to stimulate the tPA-dependent generation of plasmin from plasminogen, in the same order of magnitude (data not shown).

Initial rates of plasminogen activation were determined in the absence or in the presence of purified cartilage Ig light chains, using the plasmin substrate Chromozym-PL (Fig. 6). The data obeyed Michaelis-Menten kinetics, as demonstrated by the Lineweaver-Burk plot of the data (Fig. 6B). The addition of shark

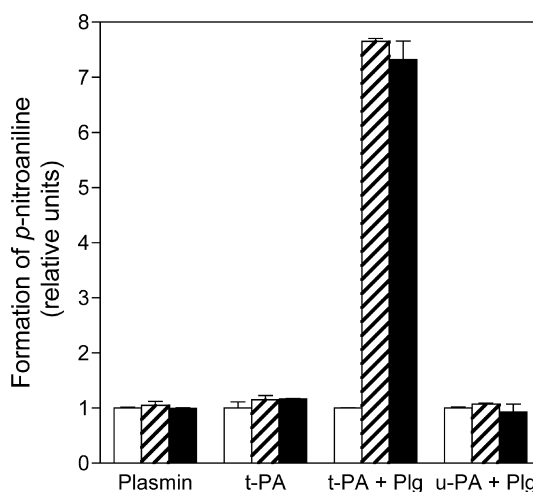


Fig. 5. Shark Ig light chains stimulate the tPA-dependent activation of plasminogen without affecting either tPA, uPA or plasmin activity. Plasmin, and tPA activities were assayed using Chromozym-PL, or Chromozym-tPA, respectively. tPA- or uPA-dependent activation of plasminogen was monitored by measuring the amidolytic activity of the plasmin generated by activation of plasminogen. All activities were measured in the absence (open bars) or in the presence of 1.25 μ g/ml Ig 4.5 (hatched bars) or Ig 6.5 (solid bars)

cartilage Ig light chain resulted in an increased dependent conversion of plasminogen in plasmin, by increasing the affinity of tPA for plasminogen by 32- and 38-fold (K_m decrease from 456 nM to 12–14 nM) but had little effect on k_{cat} (Table 2). The kinetic constants calculated are very similar for both purified Ig light chains, indicating a high degree of structural and functional identity between these two proteins.

Acceleration of fibrin degradation in vitro

Since the main physiological substrate of plasmin is fibrin, we asked whether shark Ig light chains could stimulate the degradation of a fibrin gel in the presence of the tPA/plasminogen system. As shown in Fig. 7, shark Ig light chains markedly increased the tPA/plasminogen-dependent degradation of the fibrin gel. tPA, plasminogen, or immunoglobulins alone did not significantly solubilized the fibrin gel. This activity was blocked by the serine-protease inhibitor aprotinin, suggesting that the degradation was catalyzed by the plasmin generated from plasminogen. These results confirm that shark immunoglobulins are potent stimulator of the tPA/plasminogen system, independently of the nature of the plasmin substrate.

BIAcore analysis

To determine if shark Ig light chain was directly interacting with either tPA or plasminogen or both, we proceeded to real time interaction BIAcore analysis. [Glu]Plasminogen was first immobilized on the BIAcore

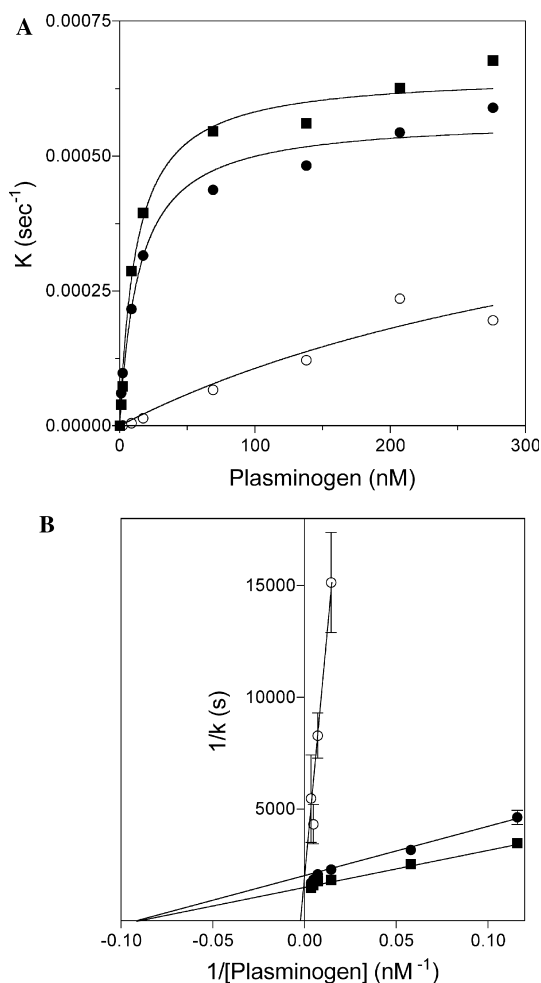


Fig. 6. Kinetic analysis of the stimulatory effect of Ig kappa light chains on tPA-dependent plasminogen activation. Activation of Glu-plasminogen (8.6–276 μM) by 5.13 nM of human tPA in the absence (○) or in the presence of 0.3 $\mu\text{g}/\text{ml}$ (11 nM) Ig 4.5 (●) or Ig 6.5 (■) was determined as described in Experimental procedures. (A) Initial rates of plasmin generation were determined from plots of A_{405} vs. t^2 , and the tPA turnover number (k) was calculated as described in Experimental procedures. (A) Experimental data were fitted to the Michaelis-Menten model by non-linear regression analysis using the Prism 4.0 software. (B) Lineweaver-Burk plot ($1/k$ vs. $1/[\text{plasminogen}]$) of the data.

Table 2

Kinetic parameters of tPA-dependent plasminogen activation in the presence of shark Ig light chains

	Control	Ig pI 4.5 (x-fold)	Ig pI 6.5 (x-fold)
K_{cat} (s^{-1})	0.000591	0.000571 (0.97)	0.000652 (1.1)
K_{m} (nM)	456	14.3 (31.8)	12.1 (37.7)

Kinetic parameters were calculated from data in Fig. 6, using non-linear regression.

sensor chip, purified shark Ig light chain was injected onto the chip surface, and sensorgrams were recorded. As shown in Fig. 8A, a strong interaction between plasminogen and shark immunoglobulins was observed, followed by a very fast dissociation at the end of the injection. Similar sensorgrams were recorded for both

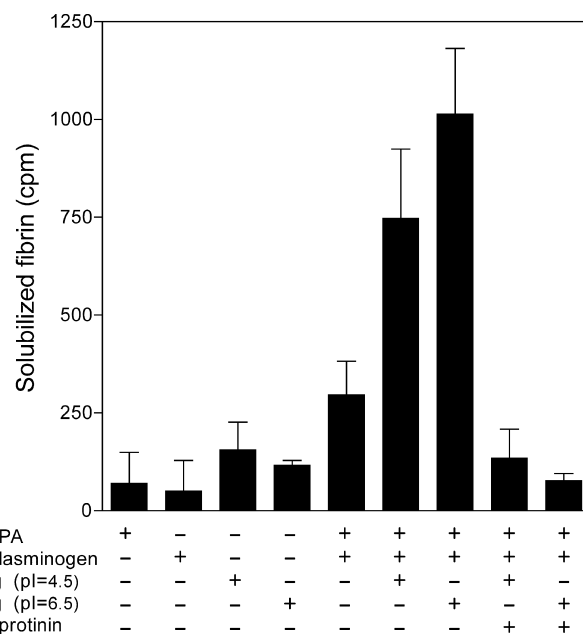


Fig. 7. Ig kappa light chains stimulate tPA/plasminogen-dependent degradation of fibrin. Fibrin gel were formed in 96-wells by mixing [^{125}I]fibrinogen with thrombin. After washing the insoluble fibrin gel, various tested proteins were added on top of the fibrin gel. After a 10-min incubation at 37 $^{\circ}\text{C}$, solubilized iodinated fibrin degradation products released in the media were quantified by γ -scintillation counting.

Ig light chains, indicating that these proteins are very similar. Table 3 shows the kinetic parameters estimated by the BIAevaluation software for the interaction between plasminogen and purified Ig light chains. The kinetic data were evaluated using both the 1:1 Langmuir binding model and the two-state conformational change model. The 1:1 Langmuir binding model was a better fit than the other model. Similar association constants ($K_{\text{A}} = 4.0 \times 10^7$ vs. $5.5 \times 10^7 \text{ M}^{-1}$) and dissociation constants ($K_{\text{D}} = 25$ vs. 18 nM) were obtained for both immunoglobulin light chains. We also performed binding assays by first immobilizing tPA on the chip and then injecting the Ig light chains or plasminogen. An interaction was monitored between Ig light chain (pI = 6.5) and tPA but the signal was weaker (approximately 100 vs. 400 RU) than for the interaction with plasminogen. Again, the 1:1 Langmuir binding model was the best fit and the association constant ($K_{\text{A}} = 2.8 \times 10^7$) and the dissociation constant ($K_{\text{D}} = 36$ nM) were determined using that model. These results clearly show that Neovastat Ig light chains stimulates plasminogen activation via a direct interaction with both plasminogen and tPA.

Discussion

Cartilage is a unique tissue as it is avascular and rarely develops malignant tumors. It was demonstrated

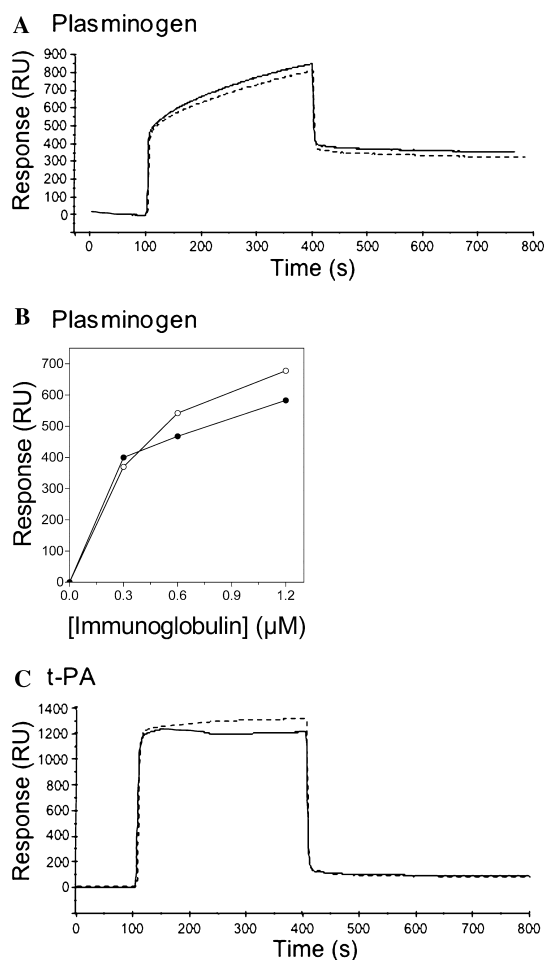


Fig. 8. Ig kappa light chains directly interact with plasminogen. Plasminogen or tPA was immobilized on a CM5 sensor chip as described in Experimental procedures. Purified shark Ig light chains were injected onto immobilized proteins at a flow rate of 5 $\mu\text{l}/\text{min}$. The surface plasma resonance response was plotted in RU as a function of time. After each injection the sensor chip surface was regenerated by injecting 10 mM glycine, pH 2.2, for 2 min. (A) Interaction between Ig light chain pI = 4.5 (solid line) or Ig light chain pI = 6.5 (dashed line) (1.2 μM) and immobilized plasminogen. (B) Increasing concentrations (0.3, 0.6, and 1.2 μM) of Ig 4.5 (○) or Ig 6.5 (●) light chain were separately injected on the chip containing immobilized plasminogen. (C) Interaction between Ig 4.5 (solid line) or Ig 6.5 (dashed line) and immobilized tPA.

in the early 1970s that cartilage contains inhibitors of angiogenesis [27], and that they can be solubilized upon homogenization in water [28]. Antiangiogenic proteins have been partially purified from shark cartilage extracts, including the 10–14-kDa U-995 [29], 18-kDa SCAF-1 [30], and the 10-kDa SCF2 [31], but the identity

of these proteins is unknown. Several inhibitors of matrix metalloproteinases have been identified in cartilage tissue from various species including TIMP-1, TIMP-2, TIMP-3 [32–34], and many TIMP-related proteins [35,36]. Examples of other classes of angiogenesis inhibitors identified in cartilage are cellular matrix protein such as chondromodulin-1 [37], thrombospondin [38], and the contractile protein troponin-1 [39].

Neovastat is an antiangiogenic agent currently undergoing Phase III clinical trials for the treatment of non-resectable non-small cell lung cancer. It is prepared by aqueous extraction of shark cartilage, followed by an ultrafiltration procedure that result in a fraction containing a variety of molecules with molecular weights of less than 500 kDa. Neovastat is thus a complex shark cartilage extract that contains anti-MMP [18], anti-VEGF [20], proapoptotic [21], and the recently described tPA stimulatory [9] activities. Because the nature of the active molecules contained in Neovastat is unknown, we made an effort to purify and identified molecules that may contribute to its antiangiogenic properties, beginning with the stimulator of the tPA-dependent conversion of plasminogen to plasmin.

Previous data showed that the tPA stimulatory activity is conserved after treatment with SDS or DTT followed by extensive dialysis [9], suggesting that denaturing purification methods such as preparative SDS-PAGE and isoelectric focusing could be used to purify the active molecules. By combining these two powerful electrophoresis methods, a separation analogous to 2D-gel electrophoresis could be achieved, but higher quantity of material can be purified, with a much better recovery. After a three-step purification procedure including gel filtration, isoelectric focusing and preparative SDS-PAGE, two 28-kDa proteins were purified to homogeneity and identified by N-terminal sequencing as Ig kappa light chains. Since the molecular size estimated by gel filtration, approximately 340 kDa, was much higher than the purified active protein, it suggest that the immunoglobulin light chain is not dissociated in Neovastat and that the whole immunoglobulin protein is able to stimulates tPA activity. At least one other stimulator of the tPA/plasminogen activity is present in Neovastat but remain identified. The most likely explanations for the failure to detect a polypeptide associated with the second peak of activity are either that it is present in very small quantity in Neovastat or that it is too small to be detected by SDS-PAGE.

Table 3

Kinetics of interaction between immobilized plasminogen or tPA and shark Ig light chains using the 1:1 Langmuir binding model

Immobilized protein	Ligand	$k_a \times 10^4$ ($\text{M}^{-1} \text{s}^{-1}$)	$k_d \times 10^{-4}$ (s^{-1})	$K_A \times 10^7$ (M^{-1})	$K_D \times 10^{-8}$ (M)
Plasminogen	Ig pI 4.5	1.2	2.9	4.0	2.5
Plasminogen	Ig pI 6.5	1.3	2.4	5.5	1.8
tPA	Ig pI 6.5	2.6	9.3	2.8	3.6

Surface-bound human IgG treated with plasmin was previously shown to binds and activates plasminogen [40]. Plasmin cleaved the whole IgG generating the Fab fragment, containing the antigen binding site, and a new COOH-terminal to which plasminogen binds [40]. In this paper, we observed a strong and rapid stimulation of plasminogen activation by shark immunoglobulins without pretreatment with plasmin or prior immobilization of the Ig light chain on a surface. The plots of Abs_{405} vs. t^2 for the activation of plasminogen by shark Ig light chains are linear for the initial rates of plasminogen. This indicates that Ig light chains have a direct and intrinsic stimulatory effect on plasminogen activation without any requirement for a preactivation by either plasmin or tPA. This contrasts with other plasminogen activators such as fibrin that exhibit a lag period during which plasmin cleaves the fibrin molecules to expose new internal lysine residues for plasminogen binding. Shark Ig light chains stimulate plasminogen activation by increasing the affinity of tPA for plasminogen (K_m decrease from 456 nM to 12–14 nM). An increased affinity of tPA for plasminogen was observed for several other plasminogen activators such as fibrin and annexin II.

Since Ig light chains bind directly to plasminogen, as demonstrated by real time protein interaction analysis on the BIAcore (Fig. 8), it is likely that the increased affinity is due to a conformational change in plasminogen that make it more readily proteolyzed by tPA. However, the fact that Ig light chains do not stimulate plasminogen activation by uPA, suggest that tPA may participate in the formation of a ternary complex with plasminogen and Ig light chain, and that the binding to plasminogen alone is not sufficient to stimulate it tPA-catalyzed conversion to plasmin. The stimulation of plasminogen activation was observed not only with a synthetic plasmin substrate but also with the more relevant physiological substrate fibrin. This result suggest that Neovastat Ig light chains may accelerate clot dissolution (fibrinolysis) by stimulating the tPA/plasminogen system. The role of tPA in tumor invasion and angiogenesis remains largely unknown. High tPA expression and activity correlates with good prognosis in melanoma and breast cancer patients, and other types of cancers [12,13 and references therein]. The mechanism involved has not been elucidated but it has been suggested that overstimulation of tPA may lead to excessive proteolysis of the provisional fibrin matrix necessary for neovessel formation, and to subsequent endothelial cell apoptosis induced by cell detachment [15]. These data suggest that the stimulation of plasminogen activation by Ig light chains contained in Neovastat may have an effect on endothelial cell adhesion *in vivo*, and thus contribute to its antiangiogenic properties.

In summary, our results identify immunoglobulin kappa light chains as a stimulator of plasmin genera-

tion, within Neovastat. Ig light chains interact with plasminogen and tPA, leading to an increased generation of plasmin. Ig light chain is the first molecule associated with the antiangiogenic properties of Neovastat to be purified and identified.

Acknowledgments

We would like to thank Nicole Lafontaine and Dr Édith Beaulieu for their technical help with some experiments. The study was supported by Æterna Laboratories, Québec City, Québec, Canada and by a grant from the Canadian Institute of Health Research (to R.B.)

References

- [1] J. Folkman, *Nat. Med.* 1 (1995) 27–31.
- [2] D. Hanahan, J. Folkman, *Cell* 86 (1996) 353–364.
- [3] M.S. Pepper, *Arterioscler. Thromb. Vasc. Biol.* 21 (2001) 1104–1117.
- [4] H.R. Lijnen, D. Collen, *Baillière's Clin. Haematol.* 8 (1995) 277–290.
- [5] G. Murphy, J. Gavrilovic, *Curr. Opin. Cell Biol.* 11 (1999) 614–621.
- [6] M.R. Gyetko, R.F. Todd III, C.C. Wilkerson, R.G. Sitrin, *J. Clin. Invest.* 93 (1994) 1380–1398.
- [7] H.Y. Min, L.V. Doyle, C.R. Vitt, L. Zandonella, J.R. Stratton-Thomas, M.A. Shuman, S. Rosenberg, *Cancer Res.* 56 (1996) 2428–2433.
- [8] D. Huber, E.M. Cramer, J.E. Kaufmann, P. Meda, J.-M. Massé, E.K.O. Kruithof, U.M. Vischer, *Blood* 99 (2002) 3637–3645.
- [9] D. Gingras, D. Labelle, C. Nyalendo, D. Boivin, M. Demeule, C. Barthelemy, R. Béliveau, *Invest. New Drugs* 22 (2004) 17–26.
- [10] M.A. Lafleur, M.M. Handsley, V. Knäuper, G. Murphy, D.R. Edwards, *J. Cell Sci.* 115 (2002) 3427–3438.
- [11] M.S. O'Reilly, L. Holmgren, Y. Shing, C. Chen, R.A. Rosenthal, M. Moses, W.S. Lane, Y. Cao, E.H. Sage, J. Folkman, *Cell* 79 (1994) 315–328.
- [12] C.M. Ferrier, S. Suci, W.L. van Geloof, H. Straatman, A.M.M. Eggermont, H.S. Koops, B.B.R. Kroon, F.J. Lejeune, U.R. Kleeberg, G.N.P. van Muijen, D.J. Ruiter, *Br. J. Cancer* 83 (2000) 1351–1359.
- [13] P.O. Chappuis, B. Dieterich, V. Sciretta, C. Lohse, H. Bonnefoi, S. Remadi, A.-P. Sappino, *J. Clin. Oncol.* (2001) 2731–2738.
- [14] R. Sawaya, O.J. Ramo, M.L. Shi, G. Mandybur, *J. Neurosurg.* 74 (1991) 480–486.
- [15] A. Reijerkerk, E.E. Voest, M.F.B.G. Gebbink, *Eur. J. Cancer* 36 (2000) 1695–1705.
- [16] D. Gingras, G. Batist, R. Béliveau, *Expert Rev. Anticancer Ther.* 1 (2001) 341–347.
- [17] G. Batist, F. Patenaude, P. Champagne, D. Croteau, C. Levinton, C. Hariton, B. Escudier, E. Dupont, *Ann. Oncol.* 13 (2002) 1259–1263.
- [18] P. Falardeau, P. Champagne, P. Poyet, C. Hariton, E. Dupont, *Semin. Oncol.* 28 (2001) 620–625.
- [19] D. Gingras, A. Renaud, N. Mousseau, E. Beaulieu, Z. Kachra, R. Béliveau, *Anticancer Res.* 21 (2001) 145–155.

- [20] R. Béliveau, D. Gingras, E.A. Kruger, S. Lamy, P. Sirois, B. Simard, M.G. Sirois, L. Tranqui, F. Baffert, E. Beaulieu, V. Dimitriadou, M.-C. Pépin, F. Courjal, I. Ricard, P. Poyet, P. Falardeau, W.D. Figg, E. Dupont, *Clin. Cancer Res.* 8 (2002) 1242–1250.
- [21] D. Boivin, S. Gendron, E. Beaulieu, D. Gingras, R. Béliveau, *Mol. Cancer Ther.* 1 (2002) 795–802.
- [22] E. Dupont, P. Falardeau, S.A. Mousa, V. Dimitriadou, M.-C. Pépin, T. Wang, M.A. Alaoui-Jamali, *Clin. Exp. Metastasis* 19 (2002) 145–153.
- [23] E. Dupont, P. Brazeau, C. Juneau, United States Patent, 5,618,925. Government Printing Office, Washington, DC, 1997.
- [24] J.C. Drapier, J.P. Tenu, G. Lemaire, J.F. Petit, *Biochimie* 61 (1979) 463–471.
- [25] M. Ranby, *Biochim. Biophys. Acta* 704 (1982) 461–469.
- [26] A.S. Greenberg, L. Steiner, M. Kasahara, M.F. Flajnik, *Proc. Natl. Acad. Sci. USA* 90 (1993) 10603–10607.
- [27] R. Eisenstein, N. Sorgente, L.W. Soble, A. Miller, K.E. Kuettner, *Am. J. Pathol.* 73 (1973) 765–774.
- [28] N. Sorgente, K.E. Kuettner, L.W. Soble, R. Eisenstein, *Lab. Invest.* 32 (1975) 217–222.
- [29] J.R. Sheu, C.C. Fu, M.L. Tsai, W.J. Chung, *Anticancer Res.* 18 (6A) (1998) 4435–4441.
- [30] X.R. Shen, D.M. Ji, F.X. Jia, X.X. Deng, J.H. Sun, X.R. Hu, D.M. Ren, *Sheng Wu Hua Xue Yu Sheng Wu Wu Li Xue Bao (Shanghai)* 32 (2000) 43–48.
- [31] J.H. Liang, K.P. Wong, in: M. Maragouchakis (Ed.), *Angiogenesis: From the Molecular to Integrative Pharmacology*, Kluwer Academic/Plenum publishers, New York, 2000, pp. 209–223.
- [32] A. Sellers, G. Murphy, M.C. Meikle, J.J. Reynolds, *Biochem. Biophys. Res. Commun.* 87 (1979) 581–587.
- [33] M. Zafarullah, S. Su, J. Martel-Pelletier, J.A. DiBattista, B.G. Costello, W.G. Stetler-Stevenson, J.P. Pelletier, *J. Cell. Biochem.* 60 (1996) 211–217.
- [34] S.S. Apte, K. Hayashi, M.F. Seldin, M.G. Mattei, M. Hayashi, B.R. Olsen, *Dev. Dyn.* 200 (1994) 177–197.
- [35] M.A. Moses, J. Sudhalter, R. Langer, *Science* 248 (1990) 1408–1410.
- [36] J.B. Murray, K. Allison, J. Sudhalter, R. Langer, *J. Biol. Chem.* 261 (1986) 4154–4159.
- [37] Y. Hiraki, H. Inoue, K. Iyama, A. Kamizono, M. Ochiai, C. Shukunami, S. Iijima, F. Suzuki, J. Kondo, *J. Biol. Chem.* 272 (1997) 32419–32426.
- [38] D.J. Good, P.J. Polverini, F. Rastinejad, M.M. Le Beau, R.S. Lemons, W.A. Frazier, N.P. Bouck, *Proc. Natl. Acad. Sci. USA* 87 (1990) 6624–6628.
- [39] M.A. Moses, D. Wiederschain, I. Wu, C.A. Fernandez, V. Ghazizadeh, W.S. Lane, E. Flynn, A. Sytkowski, T. Tao, R. Langer, *Proc. Natl. Acad. Sci. USA* 96 (1999) 2645–2650.
- [40] P.C. Harpel, R. Sullivan, T.S. Chang, *J. Biol. Chem.* 264 (1989) 616–624.